Analysis of Shortest Path Routing for Large Multi-Hop Wireless Networks

Sungoh Kwon and Ness B. Shroff

***Abstract*—In this paper, we analyze the impact of straight line routing in large homogeneous multi-hop wireless networks. We estimate the nodal load, which is defined as the number of packets served at a node, induced by straight line routing. For a given total offered load on the network, our analysis shows that the nodal load at each node is a function of the node's Voronoi cell, the node's location in the network, and the traffic pattern specified by the source and destination randomness and straight line routing. In the asymptotic regime, we show that each node's probability that the node serves a packet arriving to the network approaches the products of half the length of the Voronoi cell perimeter and the load density function that a packet goes through the node's location. The density function depends on the traffic pattern generated by straight line routing, and determines where the hot spot is created in the network. Hence, contrary to conventional wisdom, straight line routing can balance the load over the network, depending on the traffic patterns.**

***Index Terms*—multi-hop wireless network, routing, geometric probability, analysis, simulations**

I. Introduction

Over the past few years, we have witnessed a significant amount of interest in the study of ad-hoc and sensor networks. Unlike cellular networks, these networks can use other nodes as relays to deliver data from different sources to destinations. The relaying functionality makes these "multi-hop" wireless networks scalable and applicable in a variety of different areas [2]–[4].

The relaying functionality adds a complex dimension to the performance analysis of multi-hop networks. The additional traffic imposed by relaying diminishes a node's ability to transmit its own data. The relays could also induce hot spots (or congested areas) in the network, which in turn result in reducing the overall throughput in the case of battery-limited networks [5], [6]. Congestion in the hot-spot areas could also reduce the overall capacity of the wireless network [7], [8]. In [7]–[14], the authors have proposed routing algorithms to alleviate the relaying load in the congested area. However, they do not analyze the load induced by relaying traffic.

The work was supported in part by ARO MURI Award No. W911NF-07-10376 (SA08-03), NSF grants CNS 0439111, CNS 0626703, and CCF 0635202, and a grant from the Indiana 21st Century Fund. An earlier version of this paper has been presented at IEEE INFOCOM 2007 [1]

S. Kwon is with Samsung Electronics Co., Dong Suwon P.O.BOX 105, 416 Maetan-3dong, Yeongtong-gu, Suwon-si, Gyeonggi-do, 443-742, Korea (email: sungoh@ieee.org)

N. B. Shroff is with the Departments of ECE and CSE, The Ohio State University, 2015 Neil Avenue, Columbus, OH 43210, U.S.A (email: shroff@ece.osu.edu)

The analysis of the relaying traffic for homogeneous wireless network has been studied in some previous works. In [15], the authors show that in an arbitrary network[1] the load induced by relaying traffic is $O(\sqrt{n})$[2], while it is $O(\sqrt{\frac{n}{\log n}})$ for random networks[3]. In [16], the authors show that in random networks with power control the load induced by relaying traffic becomes $O(\sqrt{n})$. In [17], it is shown that the order of the relaying traffic load is independent of the traffic patterns. However, these studies in [15]–[17] focus only characterizing the performance in order terms as a function of the number of deployed nodes. From the well-known problem in mathematics called the Bertrand's paradox [18], one can show that different distributions of sources and destinations result in different distributions of the relaying load even for the same environment.

In [19], the authors analytically study the impact of shortest single-path routing on a node by approximating single paths to line segments and characterizing the deviation of routes from line segments. However, one of the parameters in their model is not analytically quantified and would need to be estimated via simulations. In [20], the authors introduce an analytical model to evaluate the imposed load at a node by approximating a shortest path route to a narrow rectangle, where the load of a node is defined as the number of paths going through that node. The length of the rectangle is defined as the distance between a source and destination and the width of the rectangle parameterizes the deviation of paths from the line segments between sources and destinations. However, since the number of nodes is not parameterized in the analytic model, the model does not provide an explicit relationship between the load and the number of nodes.

Recent work in the mobile community addressed the relaying load problem as an application of the node mobility analysis. In [21] the authors find the spatial node distribution of the random waypoint (RWP) mobility model, and extend their analytical results to traffic load induced by straight line routing in dense ad-hoc networks. However, the authors in [21] do not propose an analytic model for relay load at a given node, nor the relationship between the nodal load and the number of deployed nodes in the network. Moreover, since the probability for the existence of a node in a small element area is defined as a function of the expected length of the line

[1] An arbitrary network implies that the networks settings are arbitrary such as nodes placement, transmission range (power control) etc.

[2] We write $f(x) = O(g(x))$ to mean that $\lim_{x\to\infty} \frac{|f(x)|}{|g(x)|} < \infty$

[3] A random network implies that the networks settings are random such as nodes placement, source-destination pairs etc.

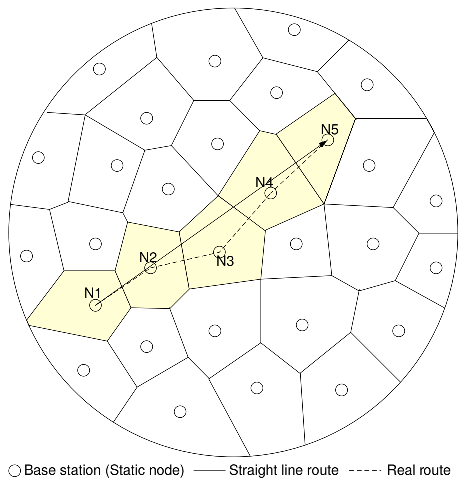

Fig. 1. Voronoi cells and a straight line routing algorithm in a two dimensional space.

segment (node's traveling distance) inside the element area in [21], we cannot directly apply the results to relaying load at a node, which is defined as a function of the expected number of the events that line segments cut the node's Voronoi cell (that will be defined in Section II) in our system model.

In this paper, we analyze the load for a homogeneous multi-hop wireless network for the case of straight line routing as in [15]–[17], [19], [20]. (Shortest path routing is frequently approximated to straight line routing in large multi-hop wireless networks [15], [22], [23]). Since geographical and geometric attributes of nodes and routes affect the nodal load, we employ results from geometric probabilities to solve the problem. Based on our analytical results, we are able to show the precise relationship between the number of nodes and the load at each node, and the geographical distribution of the relaying load over the network for different scenarios. Interestingly, straight line routing itself can balance the relay load over the disk in certain cases.

The rest of the paper is organized as follows. In Section II, we describe the system model and formulate the problem. In Section III, we analyze multi-hop wireless networks for three different source-destination random patterns. In Section IV, we study a simple form of the result that was analyzed in the previous section. In Section V, we discuss different scenarios. In Section VI, we study the properties of straight line routing and we conclude in Section VII.

II. System Models

A. Assumption

We model a multi-hop wireless network as a directed graph $G = (\mathcal{N}, \mathcal{E})$, where $\mathcal{N}$ represents the set of nodes and $\mathcal{E}$ the set of edges in the network. We assume that the wireless network is composed of n nodes on a disk $\mathcal{D}$. For simplicity, we let the radius of the disk be one, i.e., a unit disk. Each node can control its transmission range. We assume that the number of nodes is large enough and that their maximum coverage areas are overlapped in a way in which the unit disk is entirely covered by the nodes' maximum transmission coverage. Further, we assume that the nodes are totally connected. For a given deployment of nodes on a disk, we define a logical Voronoi tessellation [24] over the unit disk. There is a unique one-to-one mapping between a Voronoi cell and a node in the network. The definition is as follows. Let $\{x_1, x_2, \cdots, x_n\}$ be a set of locations of nodes in $\mathcal{N}$. The Voronoi cell $V(x_i)$ is the set of all points that are closer to x_i than to any other x_j for $j \in \mathcal{N}$, i.e.,

$$V(x_i) = \{x \in \mathcal{D} \,|\, |x - x_i| = \min_{j \in \mathcal{N}} |x - x_j|\}, \tag{1}$$

where $|x - y|$ represents a Euclidean distance between points x and y. Therefore, each node $i \in \mathcal{N}$ has its Voronoi cell v_i, which is encircled by a perimeter s_i, as in Figure 1. We assume that the probabilities that a node becomes a source and a destination are identical, and circular symmetric [4] [25]. For simplicity, unless stated otherwise, we use the perimeter of node i as a perimeter of node i's Voronoi cell throughout this paper.

B. Routing

In multi-hop wireless networks, packets are transferred through routes that could be composed of multiple relay nodes between sources and destinations. In many multi-hop wireless networks, shortest path routing is often used for its simplicity and scalability, and this is closely approximated by straight line routing for large multi-hop wireless networks. Thus, in this paper, we will focus on straight line routing for delivering packets from sources to destinations.

Straight line routing is defined as a sequence of nodes whose Voronoi cell is cut by a straight line segment between a source and destination [15]. When a packet arrives at the network, node i in the network participates in routing the packet when the straight line segment between the source and the destination cuts the perimeter s_i of node i. If two cells are simultaneously chosen as the next cell, either can be arbitrarily selected. For example, in Figure 1, a packet arriving at node N_1 is destined for node N_5. Nodes N_2, N_3, and N_4 whose perimeters cut by a line segment between N_1 and N_5 will participate in routing the packet.

C. Nodal Load and Problem Formulation

We define the *nodal load* as the expected number of packets that traverse the node (as in [15], [19], [20]). For a given total offered load on the network, M, the nodal load L_i at node i can be expressed as

$$\begin{aligned} L_i &= E[\text{the number of packets served by node } i] \\ &= M p_i, \end{aligned} \tag{2}$$

where p_i represents the probability that a packet goes through node i. We say that loads are *balanced* when all the nodal loads are identical, i.e., there exists p such that

$$p_i = p \;\forall i \in \mathcal{N}.$$

[4] The probability density function of a random variable $X \in \mathcal{R}^2$ is circular symmetrical if it depends only on the Euclidean distance $|X|$ from the origin.

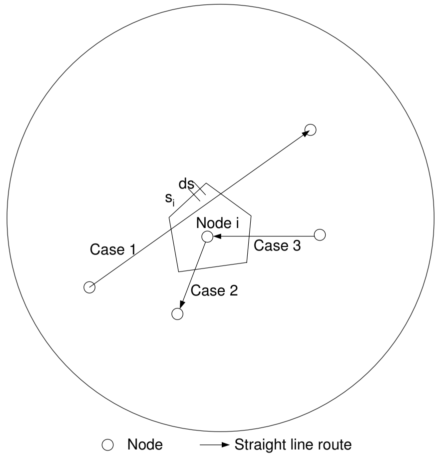

Fig. 2. Node i will participate in routing when a line segment between a source and destination cuts its perimeter s_i.

To find p_i in (2), recall that v_i is the Voronoi cell of node i, which is encircled by perimeter s_i. Node i will participate in routing a packet when the line segment between the source and destination cuts its perimeter s_i, and there are three cases depending on the locations of the source and destination, as shown in Figure 2. In the case of a relay (Case 1 in Figure 2), a line segment cuts s_i at exactly two points. Otherwise, the perimeter is cut by a line segment at one point, i.e., Cases 2 and 3 in Figure 2 (the probability of the set of outcomes with a line touching a corner or lying congruent with a side of the polygon is zero). Since the probabilities that node i becomes a source and a destination are identical (from our assumption), we have

$$\begin{aligned} p_i &= \Pr\{\text{Node } i \text{ becomes a relay or a source}\} \\ &= \frac{1}{2}\int_{s\in s_i} f(s)ds, \end{aligned} \tag{3}$$

where $f(s)$ is the load density function that a line segment between a source and destination goes through point s. In other words, we can interpret $f(s)$ as the relaying load that a packet arriving to the network is relayed at s using straight line routing. When a node is a pure relay node that does not generate or drain packets, (3) is exactly the probability that node i becomes a relay. If we know $f(s)$ in (3), we can find p_i to estimate the load on node i. However, the load density function $f(s)$ depends on the traffic patterns, which are a function of the sources and destinations activated. Since we assume that homogeneous nodes are uniformly distributed over the disk, the statistical geometry of the Voronoi cells are identical. From (3), we can say that the relay load is balanced when the load density function is constant on domain $[0, 1)$.

In the next section, we study how traffic patterns affect the load density function that decides the nodal load at each node.

III. Traffic Patterns versus Load Density

In this section we characterize the load density function in (3) for three different scenarios. For the scenarios, we consider two kinds of system settings. The first system setting corresponds to uniformly distributed source-destination pairs on a disk. Most previous works study on the network performance based on this assumption [15], [19], [20].

The other setting we study is when source-destination pairs are distributed only on the circumference of a circle. Here, we will consider two different traffic models, hence we consider a total of three different scenarios. The motivation for this study comes from the following. To enhance network performance, large wireless networks use a cluster-based structure [26]. A cluster is defined as a set of nodes that are relatively close to each other. In the clustered system model, source-destination pairs (S_o and T_o) are located out of the cluster area and line segments randomly lay on the cluster, as in Figure 3. The line segments going through the cluster area can be specified by source-destination pairs (S and T in Figure 3) on the perimeter of the cluster area corresponding to S_o and T_o. Hence, we can model traffic patterns with source-destination pairs (S and T) on the perimeter of the cluster no matter what shape of the entire network and traffic patterns are. We assume that the cluster area is a unit disk and that source-destination pairs (S and T) are located only on the perimeter. The case when gateways are uniformly distributed on the perimeter of the circle, called the border gateways model in [27], also falls into this category. For this cluster model, we do not consider the cluster heads in [28]. Our interest in this paper is how the relay traffic will be distributed across the network when sources and destination are densely located on the border of a disk-like network and the relays are uniformly distributed on the disk. The cluster system model has more of a theoretical interest and the analytical results give some insight into straight line routing.

As mentioned above, we consider two different traffic models for this system setting. Since different traffic models create different load distributions over the network even in the same system setting, we separately handle the two traffic models as two independent problems. The applicability of the models depends on how network engineers establish a model for random traffic in the field. In the first traffic model, the source-destination pairs (S and T in Figure 3) are uniformly chosen on the circular perimeter of the cluster. In the second model, the distance (ψ in Figure 3) and angle (ϕ in Figure 3) of a random chord are uniformly distributed on $[0, 1)$ and $[0, 2\pi)$, respectively. We summarize the models in Table I. Since the second system setting is simpler than the first one, in Section III-A we will begin with the second one.

In all the scenarios described earlier we follow the procedures outlined below to find the load density function $f(s)$, where the distance from the origin to point s is r:

1) Find the points on a circle with radius r cut by a line segment between a source and destination and count the number of the points, χ_r, since geometric properties are invariant of angle ϕ.
2) Find the expected number of points on a circle with radius r cut by the line segment, $E[\chi_r]$.
3) Since the probability that a point on a circle is cut by line segments is identically distributed on the circle, divide the expected number of points by the perimeter length, $2\pi r$, to find the load density function $f(s)$.

For step (2) in the above procedures, we use previously derived

TABLE I
SYSTEM MODELS AND TRAFFIC MODELS

Scenario (Section)	System model	Random traffic model
1 (III-A)	Cluster	Uniformly distributed source-destination pairs on the circumference
2 (III-B)	Cluster	Uniform distance to origin and uniform angle with axis
3 (III-C)	Entire	Uniformly distributed source-destination pairs on the disk

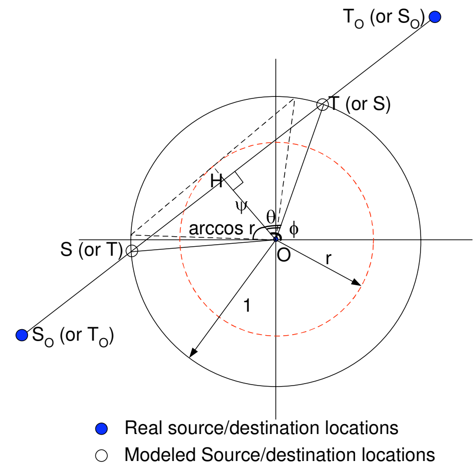

Fig. 3. In the case when source-destination pairs are located out of a disk. ψ is the length of line segment $\overline{OH}$. θ is half an angle of $\angle SOT$, i.e. $\angle SOH$. ϕ is an angle between $\overline{OH}$ and x-axis.

results studied from geometric probability [18].

To verify our analysis, we compare it with simulation results for each scenario. For the simulations, we generate 10^4 source-destination pairs and line segments between the pairs according to random traffic models, and average five simulation results with different random seeds.

A. Scenario 1: When source-destination pairs are uniformly distributed on the perimeter of a circle

Let random variable $X \in \mathcal{R}^2$ be the location of a source or a destination and Φ be a random variable that is uniformly distributed between 0 and 2π. The location is represented as

$$x = (\cos\phi, \sin\phi) \text{ for } 0 \le \phi \le 2\pi.$$

Then, the generated random chord between a source and destination can be specified by a half angle Θ ($\angle HOS$ or $\angle HOT$) between two points, as in Figure 3. The half angle Θ is also a random variable with domain $[0, \frac{\pi}{2})$. From [18, page 138], $f_\Theta(\theta)$, the probability density function of Θ is

$$f_\Theta(\theta) = \frac{2}{\pi} \text{ for } 0 \le \theta \le \frac{\pi}{2}. \tag{4}$$

For given radius r, the number of points χ_r at which a circle with radius r meets a chord is given by

$$\chi_r = \begin{cases} 2, & \arccos(r) \le \theta \le \frac{\pi}{2} \\ 0, & \text{otherwise.} \end{cases}$$

For a given θ, the conditional expectation of χ_r is

$$E[\chi_r|\theta] = \begin{cases} 2, & \arccos(r) \le \theta \le \frac{\pi}{2} \\ 0, & \text{otherwise.} \end{cases} \tag{5}$$

From (4) and (5), the expected number of points that a chord intersects a circle with radius r for $0 \le r \le 1$ is

$$\begin{aligned} E[\chi_r] &= E[E[\chi_r|\Theta]] \\ &= \int_0^{\frac{\pi}{2}} E[\chi_r|\theta] f_\Theta(\theta) d\theta \\ &= \frac{4}{\pi} \arcsin(r). \end{aligned}$$

Hence, the load density that a chord meets a point, $s \in \mathcal{D}$, is

$$f(s) = \frac{E[\chi_r]}{2\pi r} = \frac{2 \arcsin r}{\pi^2 r},$$

where r is the distance from s to the origin. Note that when θ is $\arccos(r)$, the chord meets a circle with radius r at one point, as in Figure 3, but the probability is zero in this case.

Figure 4 (a) shows the expected number of points at which a chord generated by a pair of source and destination nodes intersects a circle with radius r. Figure 4 (b) shows the load density that the chord intersects a point on a circle with radius r for $0 \le r \le 1$. As can be seen in Figure 4, in contrast to the traffic model generated by random source-destination pairs on a disk [19], [20], the outskirts of the disk have more traffic than the center area of the disk. Hence, network performance, such as throughput, depends on the nodes on the outskirts of the disk.

B. Scenario 2: Uniform distance to origin and uniform angle with axis

Any straight line segment that goes through $\mathcal{D}$ is completely specified by the distance (ψ) and direction (ϕ) of the line segment from the center of the circle to the midpoint of the chord, as in Figure 3. We let the distance and the angle (direction) of the chord be random variables that are uniformly distributed on $[0, 1)$ and $[0, 2\pi)$, respectively. As in the previous subsection, the generated random chord between a source and destination can be specified by a half angle Θ between two points. The half angle Θ is also a random variable with domain $[0, \frac{\pi}{2})$. From [18, page 139], $f_\Theta(\theta)$, the probability density function of Θ, is given by

$$f_\Theta(\theta) = \sin\theta, \text{ for } 0 \le \theta \le \frac{\pi}{2}. \tag{6}$$

For given radius r, the number of points χ_r that a circle with radius r meets a chord is

$$\chi_r = \begin{cases} 2, & \arccos(r) \le \theta \le \frac{\pi}{2} \\ 0, & \text{otherwise.} \end{cases}$$

For a given θ, the conditional expectation of χ_r is

$$E[\chi_r|\theta] = \begin{cases} 2, & \arccos(r) \le \theta \le \frac{\pi}{2} \\ 0, & \text{otherwise.} \end{cases} \tag{7}$$

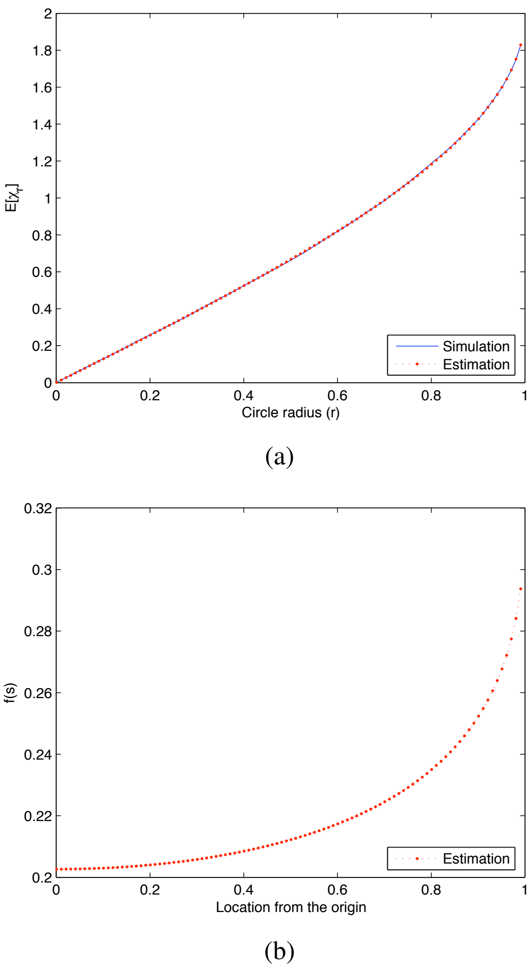

Fig. 4. Scenario 1: (a) The expected number of points at which a chord intersects a circle with radius r (b) Load density that a chord intersects a point on a circle with radius r

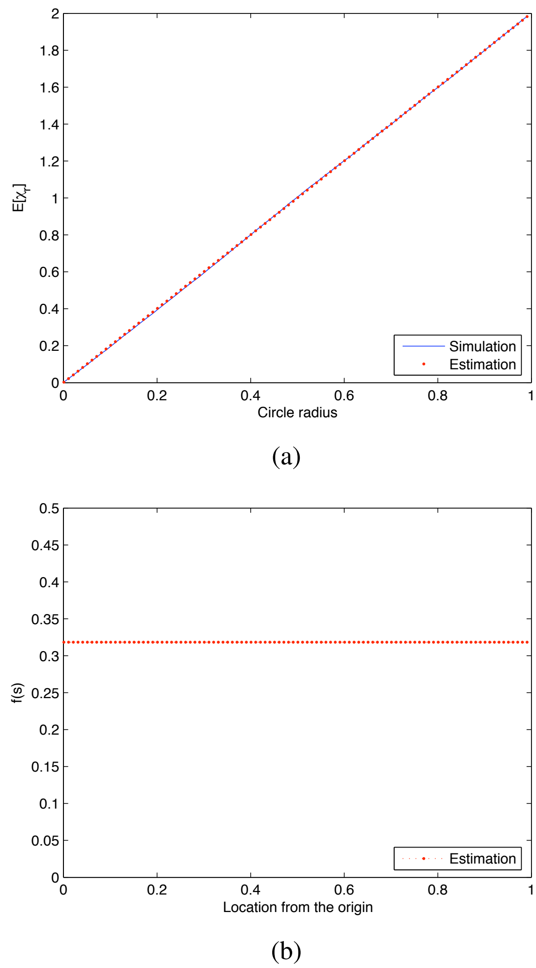

Fig. 5. Scenario 2: (a) The expected number of points at which a chord intersects a circle with radius r (b) Load density that a chord intersects a point on a circle with radius r

From (6) and (7), the expected number of points that a chord intersects a circle with radius r for $0 \leq r \leq 1$ is

$$\begin{aligned} E[\chi_r] &= E[E[\chi_r|\Theta]] \\ &= \int_0^{\frac{\pi}{2}} E[\chi_r|\theta] f_\Theta(\theta) d\theta \\ &= 2r. \end{aligned}$$

Hence, the load density that a chord meets a point, $s \in \mathcal{D}$, is

$$f(s) = \frac{E[\chi_r]}{2\pi r} = \frac{1}{\pi}, \tag{8}$$

where r is the distance from s to the origin.

Figure 5 (a) shows the expected number of points at which a chord generated by a pair of source and destination nodes, intersects a circle with radius r. Figure 5 (b) shows the load density that the chord intersects a point on a circle with radius r for $0 \leq r \leq 1$. Even in the same system setting as Scenario 1, $E[\chi_r]$ and $f(s)$ of Scenario 2 have different shapes from those of Scenario 1.

Another approach: Using the characteristic of line randomness, we can find the same solution as (8) from previous studies on geometric probability in [18], [29]. In particular, from [18], [29] we have the following theorem.

Theorem 1: Let K_0 be a convex set in a plane. We assume that lines randomly placed in the plane are isotropic and uniformly distributed. Then, for any convex set K_1 such that $K_1 \subset K_0$, the probability that a random line intersects set K_1 given that the line intersects set K_0 is

$$\Pr[\text{line hits } K_1|\text{hits } K_0] = \frac{l_{K_1}}{l_{K_0}},$$

where l_{K_1} and l_{K_0} be the perimeters of K_1 and K_0, respectively.

Disk $\mathcal{D}$ is a convex set. Voronoi cells $V(x_i)\ \forall i \in \mathcal{N}$ defined in (1) are convex sets [30] and subsets of disk $\mathcal{D}$. Since random lines in Scenario 2 are isotropic and uniformly distributed, from Theorem 1, the probability that node i becomes a relay is as follows:

$$\begin{aligned} p_i &= \Pr[\text{line hits node } i\text{'s Voronoi cell}|\text{hits disk } \mathcal{D}] \\ &= \frac{\text{the perimeter of node } i\text{'s Voronoi cell}}{\text{the perimeter of disk } \mathcal{D}} \\ &= \frac{l_{s_i}}{2\pi} \end{aligned}$$

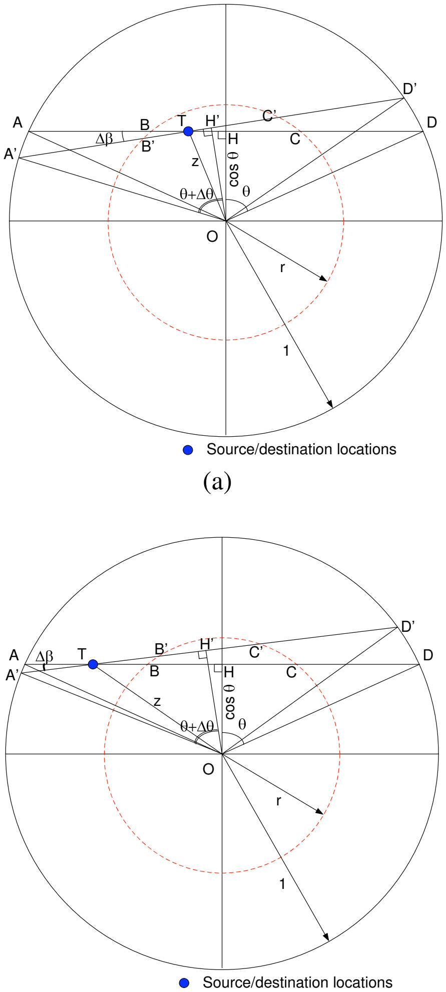

Fig. 6. When source-destination pairs are uniformly distributed on a disk: (a) node T is in a circle with radius r (b) node T is out of a circle with radius r

$$= \frac{1}{2}\int_{s\in s_i} \frac{1}{\pi} ds, \tag{9}$$

where l_{s_i} is the perimeter of node i's Voronoi cell.

From (9), we have the same density as (8) such that, for $s \in \mathcal{D}$,

$$f(s) = \frac{1}{\pi}.$$

C. Scenario 3: When source-destination pairs are uniformly distributed on a disk

Let R and Φ be uniformly distributed random variables over $[0, 1)$ and $[0, 2\pi)$, respectively. Let random variable $X \in \mathcal{R}^2$ be the location of a source or a destination uniformly distributed over a disk with radius one, then the location is represented as

$$x = (\sqrt{r}\cos\phi, \sqrt{r}\sin\phi),$$

where $0 \le r \le 1$ and $0 \le \phi < 2\pi$ [31]. The probability density function that a point randomly picked in the unit disk is located at distance z from the center is

$$f_Z(z) = 2z, \text{ for } 0 \le z \le 1. \tag{10}$$

In the case when source and destination pairs are randomly chosen on the unit disk, in contrast to the previous cases, we cannot specify line segments between sources and destinations cutting a circle only with half angles. Depending on the locations of the two nodes, the number of points χ_r on the circle with radius r cut by the line segment between two nodes are different. Hence, we first fix a node whose distance from the center is z, and denote that node by T. For the given node T, we find the conditional probability density function of the half angle of a chord and the conditional expectation of the number of points χ_r.

We denote A (A') and D (D') as the end points of a chord with a half angle θ ($\theta + \Delta\theta$), and B (B') and C (C') as the points on a circle cut by the chord $\overline{AD}$ ($\overline{A'D'}$). We denote $\Delta\beta$ as the acute angle between two chords $\overline{AD}$ and $\overline{A'D'}$ that meet at T. Two wedged regions, TAA' and TDD', made by the two chords are denoted by $\mathcal{A}$ and $\mathcal{B}$, respectively.

Given that the first random node T falls a distance z from the center of the unit disk, as in Figures 6 (a) and 6 (b), the probability that the chord going through the two random points intercepts an arc of half angle between θ and $\theta + \Delta\theta$ is the probability that the second point S falls in two wedged regions $\mathcal{A}$ and $\mathcal{B}$. For $0 \le \theta \le \frac{\pi}{2}$, the conditional probability is

$$\begin{aligned} &\Pr[(\theta, \theta + \Delta\theta)|z] \\ = \ &\frac{2}{\pi}(z^2 - \cos^2\theta + \sin^2\theta)\frac{\sin\theta\Delta\theta}{\sqrt{z^2 - \cos^2\theta}}, \end{aligned} \tag{11}$$

where chords with half angles θ and $\theta + \Delta\theta$ meet with angle $\Delta\beta$. Hence, the conditional probability density function of θ for $0 \le \theta \le \frac{\pi}{2}$ is

$$\begin{aligned} &f_{\Theta|Z}(\theta|z) \\ = \ &\lim_{\Delta\theta\to 0} \frac{\Pr[(\theta, \theta + \Delta\theta)|z]}{\Delta\theta} \\ = \ &\frac{2\sin\theta(z^2 - \cos^2\theta + \sin^2\theta)}{\pi\sqrt{z^2 - \cos^2\theta}}. \end{aligned} \tag{12}$$

Given radius r, depending on the locations of random points T and S on the unit disk, there exist three cases. First, the line segment does not meet the circle with radius r. Second, the line segment does meet the circle with radius r at one point. Finally, the line segment meets the circle with radius r at two points.

The number of points χ_r on a circle with radius r cut by the line segment between two nodes S and T, is

$$\chi_r = \begin{cases} 2, & \{r \le z \le 1 \text{ and } S \in \mathcal{B}_{b3}\} \\ 1, & \{r \le z \le 1 \text{ and } S \in \mathcal{B}_{b2}\} \\ & \bigcup\{0 \le z \le r \text{ and } S \in \mathcal{A}_{a1} \bigcup \mathcal{B}_{a1}\} \\ 0, & \text{otherwise}, \end{cases}$$

where $\mathcal{A}_{a1}$ and $\mathcal{B}_{a1}$ are regions $ABB'A'$ and $CDD'C'$ in Figure 6 (a), respectively, in the case of $z \le r$. In the case of $r \le z \le 1$, we let $\mathcal{B}_{b2}$ and $\mathcal{B}_{b3}$ denote regions $BCC'B'$ and $CDD'C'$ in Figure 6 (b), respectively.

In the case when the first node T falls in the circle with radius r, given distance z and angle $(\theta, \theta + \Delta\theta)$, the conditional expectation of the number of points χ_r is

$$E[\chi_r|(\theta,\theta+\Delta\theta),z] = 1\times\frac{\text{Area}(\mathcal{A}_{a1}\bigcup\mathcal{B}_{a1})}{\text{Area}(\mathcal{A}\bigcup\mathcal{B})} = \frac{(1-r^2)}{(z^2-\cos^2\theta+\sin^2\theta)}, \quad (13)$$

where Area($\mathcal{A}$) represents the area of region $\mathcal{A}$.

In the case when the first node T falls out of the circle with radius r, given distance z and angle $(\theta,\theta+\Delta\theta)$, the conditional expectation of the number of points χ_r is

$$\begin{aligned} & E[\chi_r|(\theta,\theta+\Delta\theta),z] \\ = \; & 1\times\frac{\text{Area}(\mathcal{B}_{b2})}{\text{Area}(\mathcal{A}\bigcup\mathcal{B})}+2\times\frac{\text{Area}(\mathcal{B}_{b3})}{\text{Area}(\mathcal{A}\bigcup\mathcal{B})} \\ = \; & \frac{(1-r^2+2\sin\theta\sqrt{z^2-\cos^2\theta})}{(z^2-\cos^2\theta+\sin^2\theta)}. \end{aligned} \quad (14)$$

The details of (11), (13), and (14) are given in Appendix.

The chords whose half angle is between $\arccos r$ and $\frac{\pi}{2}$ can intersect the circle with radius r. Given $\theta\in(\arccos r,\frac{\pi}{2})$, the first node T falls in the region such that the distance z from the center is between $\cos\theta$ and 1. From (13) and (14), the conditional expectation of χ_r is

$$E[\chi_r|\theta,z] \quad (15)$$
$$= \begin{cases} \frac{(1-r^2)}{(z^2-\cos^2\theta+\sin^2\theta)}, & \{\cos\theta\le z\le r \\ & \text{and } \arccos r\le\theta\le\frac{\pi}{2}\} \\ \frac{(1-r^2+2\sin\theta\sqrt{z^2-\cos^2\theta})}{(z^2-\cos^2\theta+\sin^2\theta)}, & \{r\le z\le 1 \\ & \text{and } \arccos r\le\theta\le\frac{\pi}{2}\} \\ 0, & \text{otherwise.} \end{cases}$$

We are now ready to obtain the expected number of points on the circle with radius r cut by the line segments between two random nodes. From (10), (12) and (15), we have

$$\begin{aligned} & E[\chi_r] \\ = \; & E[E[\chi_r|\Theta,Z]] \\ = \; & \int_{\{\cos\theta\le z\le 1,\ \arccos r\le\theta\le\frac{\pi}{2}\}} E[\chi_r|\theta,z]f_{\Theta|Z}(\theta|z)f_Z(z)dzd\theta \\ = \; & \frac{4}{\pi}(1-r^2)(\arcsin r+r\sqrt{1-r^2}). \end{aligned}$$

Hence, the load density function that the line segment between a source and destination goes through a point $s\in\mathcal{D}$ is

$$f(s) = \frac{E[\chi_r]}{2\pi r} = \frac{4}{2\pi^2}(1-r^2)\left(\frac{\arcsin r}{r}+\sqrt{1-r^2}\right),$$

where r is the distance from s to the origin.

Figure 7 shows that our analysis is identical to the simulation results. These results confirm that the hot spot is located near the center area, as in [19], [20]. The load density function has a different shape from the previous subsections. However, given that we have three different hot spots for different traffic patterns, this suggests that the hot spot area depends on the traffic pattern specified by how the source-destination pairs are distributed.

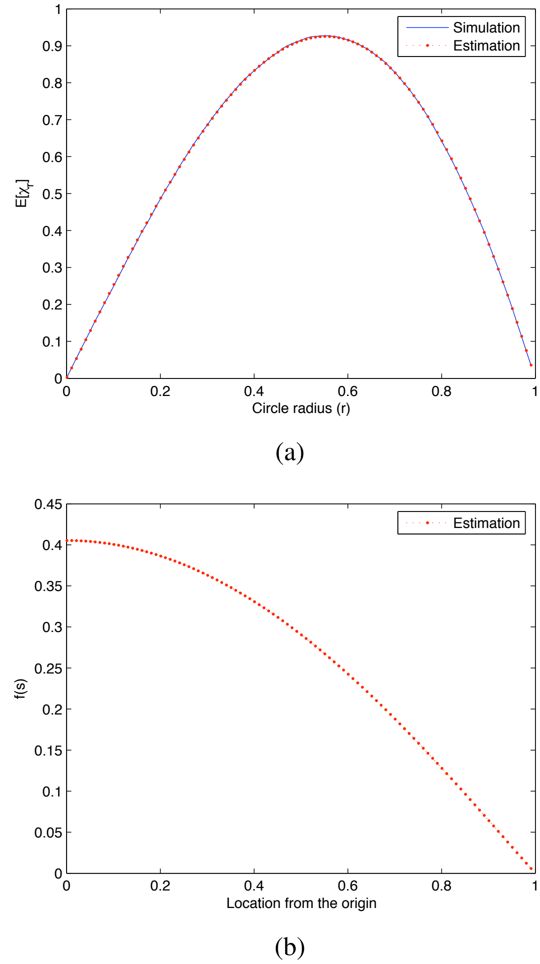

Fig. 7. Scenario 3: (a) The expected number of points at which a chord intersects a circle with radius r (b) Load density that a chord intersects a point on a circle with radius r

IV. Approximation and Convergence

From the results of the previous sections, we can compute the probability that a node will participate in routing when a packet arrives at the network for a given location, perimeter, and traffic pattern. The probability is not expressed in a closed form. However, in the asymptotic regime, we can approximate the probability by a simple closed form expression. The approximated form gives us an understanding of network performance under various environments.

When the network gets denser, the perimeters of nodes grow smaller so that the load density function on the perimeter can be approximated by the load density function at the node's location. Hence we can express (3) as

$$p_i = \frac{l_{s_i}}{2}f(x_i)+e_i, \quad (16)$$

where l_{s_i} represents the total length of the perimeter s_i of node i and e_i is an error between the exact value and the approximated value at node i.

We show here that the error between (3) and (16) converges to zero as the Voronoi cell goes to zero, i.e., the number of nodes goes by infinity. We assume that node i is located at x_i

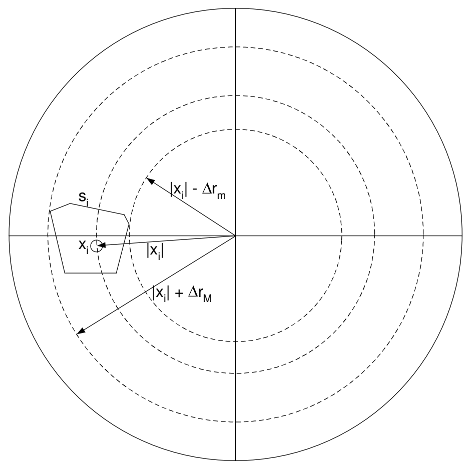

Fig. 8. When node i is located at x_i and has a perimeter s_i.

and has a Voronoi cell s_i, as illustrated in Figure 8. We define Δr_m and Δr_M as

$$\Delta r_m = \max_{s \in s_i} (|x_i| - |s|) \text{ and } \Delta r_M = \max_{s \in s_i} (|s| - |x_i|),$$

where $\Delta r = \max\{\Delta r_m, \Delta r_M\}$. When Δr is small, from Taylor's series [32], the error at node i, e_i, is

$$\begin{aligned} e_i &= \left| \frac{1}{2} \int_{s \in s_i} f(s) ds - \frac{1}{2} \int_{s \in s_i} f(x_i) ds \right| \\ &\leq \frac{1}{2} \int_{s \in s_i} |f(s) - f(x_i)| ds \\ &= O(\Delta r^2). \end{aligned} \tag{17}$$

Since Δr^2 decreases linearly as n increases, (17) shows that the error between our approximation and the exact value will decrease as n increases.

Figures 9, 10, and 11 show the comparison of our approximation and simulation results. We assume that each node has a circular Voronoi cell. We vary the number of nodes from 100 to $10,000$ and observe the probability that a packet goes through a node located at $(0, 0.5)$. For illustration, we generate 0.1 million packets per simulation and run 25 simulations with different random seeds. The error bars represent the 98% confidence levels centered around the mean values. As the number of deployed nodes goes to infinity, the probability that a node takes part in routing packets inversely increases as expected. This implies that for a given distribution of sources and destinations, and node location, the probability only depends on the length of the perimeter. As shown in Figures 9, 10, and 11, the approximation is close to the simulation results and improves as the density of nodes increases. Hence, in the case when the network is dense, the probability that a node can serve a packet can be precisely computed by our analytical results.

V. Implication of Straight Line Routing in Multi-hop Wireless Routing

We now study how our analytical results apply for estimating network performance in different environments. Unlike

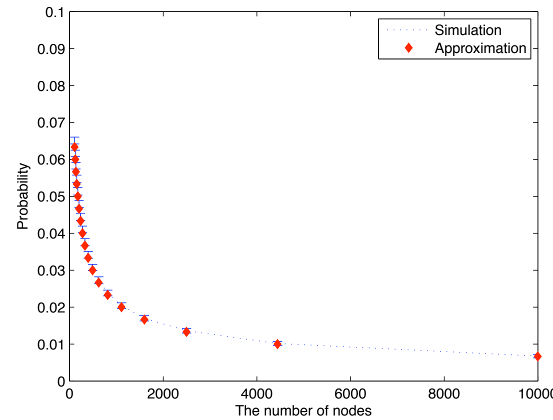

Fig. 9. When node i is located at (0,0.5) and a pair of a source and destination are uniformly distributed on a circle

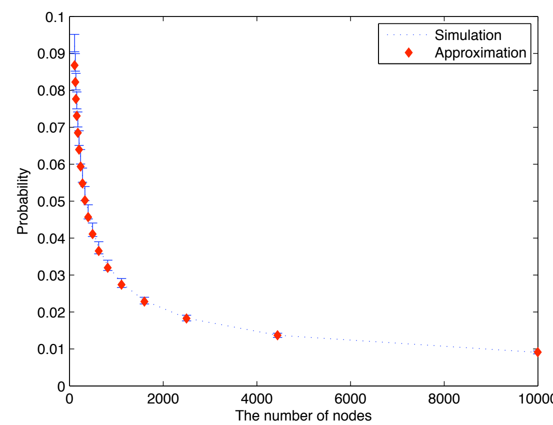

Fig. 10. When node i is located at (0,0.5) and the distance and the angle of a chord are uniformly distributed

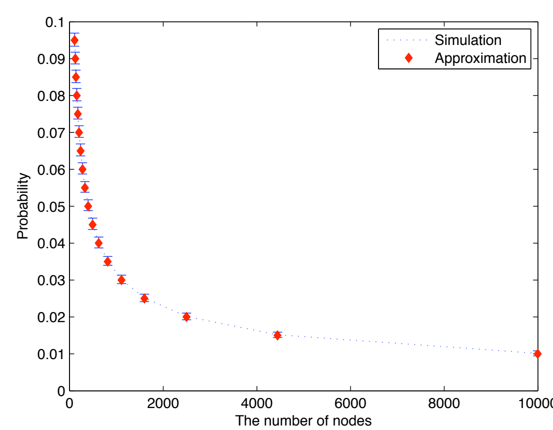

Fig. 11. When node i is located at (0,0.5) and a pair of a source and destination are uniformly distributed on a disk

previous works that study the performance order [15]–[17] or estimate the performance with parameters that need to be obtained via simulations [19], [20], we estimate the performance for a given traffic pattern by using our analytical results. Note that the uniform distribution we have assumed can be approximated by a Poisson distribution[5] and the average length of a Voronoi cell for a homogeneous Poisson point process is $\frac{4}{\sqrt{\rho}}$, where ρ is the average number of points per unit area [34]. Hence, we assume that the half length of the perimeter is $\frac{2\sqrt{\pi}}{\sqrt{n}}$, where n is the number of nodes uniformly deployed on a unit disk.

A. Nodal load in the case of homogeneous nodes

We assume that new packets arrive at each node with arrival rate λ and that the arrival distributions are independent and identically distributed. The packet arrival rate at node i is equal to $\lambda n p_i$. Hence, we can express the load of node i per unit time as

$$\begin{aligned} & \text{The load of node } i \text{ located at } x_i \\ = \;& n\lambda p_i \\ = \;& \lambda n \left(\frac{l_{s_i}}{2} f(x_i) \right) \\ = \;& \lambda n \left(\frac{2\sqrt{\pi}}{\sqrt{n}} f(x_i) \right) \\ = \;& 2\sqrt{\pi}\lambda f(x_i)\sqrt{n}. \end{aligned}$$

Hence, when the number of deployed nodes, n, increases, the load at each node becomes $O(\sqrt{n})$, which is consistent with the results in [15], [17]. In contrast to [15], [17], our analytical result can capture the load variance that depends on the location in the network.

B. Nodal load in the case of pure relay nodes

Unlike the previous subsection, we consider the case when n nodes generate data and m nodes contribute only to relaying packets. The packet arrival rate at each node is λ, then the load of node i per unit time is formally expressed as

$$\begin{aligned} & \text{The load of node } i \text{ located at } x_i \\ = \;& n\lambda p_i \\ = \;& \lambda n \left(\frac{l_{s_i}}{2} f(x_i) \right) \\ = \;& \lambda n \left(\frac{2\sqrt{\pi}}{\sqrt{n+m}} f(x_i) \right) \\ = \;& 2\sqrt{\pi}\lambda f(x_i) \left(\frac{n}{\sqrt{n+m}} \right). \end{aligned}$$

Hence, when the number of deployed nodes, n, is dominant, the load at each node increases as $\sqrt{n}$. For a given nodes n, the pure relay nodes mitigate the total load on the order of $\frac{1}{\sqrt{m}}$.

[5] Suppose there exists exactly one event of a Poisson process by time t. Then, the time at which the event occurred is uniformly distributed over $[0, t]$ [33]. We can also extend the result to the 2 dimensional case.

C. Throughput of Straight Line Routing

The definition of throughput in a multi-hop wireless network could depend on the network scenario and application being considered (e.g., [6], [35]–[38]). As in [6], [36], [38], we define *throughput* of a battery-limited multi-hop wireless network as the total number of packets served by the network until the first node dies.

When each node has an initial amount of energy E^{init} and e_p is the energy consumed to deliver a packet to the next node, the network can serve $\frac{E^{init}}{e_p p_i}$ packets until node i located at x_i dies.

The throughput of the network can be expressed as

$$\begin{aligned} & \text{Throughput of the network} \\ = \;& \min_{i \in \mathcal{N}} \frac{E^{init}}{e_p p_i} \\ = \;& \left(\frac{E^{init}}{2\sqrt{\pi} e_p} \right) \sqrt{n} \left(\min_{x_i \in \mathcal{D}} \frac{1}{f(x_i)} \right), \end{aligned} \tag{18}$$

where disk $\mathcal{D}$ is a domain of x_i. With straight line routing, in the case when e_p is fixed and a source-destination distribution is given, the throughput of the network becomes $O(\sqrt{n})$ as the number of node increases. Even though the deployed number is fixed, the throughput in (18) depends on the source-destination pattern $f(x_i)$.

VI. Myths of Straight Line Routing

There have been three traditionally believed myths about straight line (or shortest path) routing for multi-hop wireless networks. These are:

1) Straight line routing results in congested areas, and load balancing is needed to alleviate it.
2) A congested area induced by straight line routing is located at the center of the network.
3) Equalizing the load across each link (equal load balancing) always helps improve network performance.

Using the analysis results in Sections III and IV, we discuss the properties of straight line routing, and study the relationship between straight line routing and "equal load-balance routing" based on our analytical results.

Before starting our discussion on straight line routing, we clearly specify the definition of equal load-balancing routing. We define *load-balancing routing* as routing that makes all nodal loads equal over the network [19], [20] such that, as explained in Section II-C,

$$p_i = p \;\forall i \in \mathcal{N} \text{ and } p \in [0, 1).$$

Since homogeneous nodes are uniformly distributed on the disk, each Voronoi cell has statistically identical properties. As shown in Section IV, the approximation of a nodal load is asymptotically tight and the density $f(s)$ determines the nodal load in the asymptotic regime. Hence, we can characterize the properties of straight line routing.

TABLE II

SUMMARY OF STRAIGHT LINE ROUTING: $f(s)$ STANDS FOR THE LOAD DENSITY THAT A LINE SEGMENT GOES THROUGH POINT $s \in \mathcal{D}$ AND r REPRESENTS THE EUCLIDEAN DISTANCE BETWEEN THE ORIGIN AND POINT s. A CONGESTED AREA IMPLIES AN AREA THAT HAS MORE LOAD THAN ANY OTHER AREA IN THE NETWORK.

Scenario (Section)	$f(s)$	Congestion area	Load-balancing routing
1 (III-A)	$\frac{2\arcsin r}{\pi^2 r}$	boundary	may hurt
2 (III-B)	$\frac{1}{\pi}$	nowhere	the same
3 (III-C)	$\frac{4}{2\pi^2}(1-r^2)\left(\frac{\arcsin r}{r}+\sqrt{1-r^2}\right)$	center	may help

A. Paradox of straight line routing

As summarized in Table II, the relay load distributions depend on the system models and the generated traffic patterns. Even if the system settings and the routing schemes are identical, the different traffic patterns generated by sources and destinations result in the different distributions of relaying load, as shown by Bertrand's paradox [18].

In the first scenario considered (Section III-A), the load at the edge area is heavier than any other area so that the traffic is more congested on the fringe of the network. In the second scenario (Section III-B), straight line routing distributes the load evenly over the network, and hence does not induce hot spots. Only Scenario 3 in Section III-B corresponds to the case that straight line routing induces a congested area at the center of the network.

B. Straight line routing versus Load-balancing routing

It has been traditionally believed that shortest path (or straight line) routing could lead to hot spots in the network, degrading the network performance. Hence, load balancing algorithms have been developed to evenly distribute the load over the network to enhance network performance [5]–[14], [19], [20]. For example, in [5], [6], equally balanced load in terms of residual energy lengthens the network's life span. However, load-balancing *may not* help improve network performance.

In the case of Scenario 1, the load at the edge area is the heaviest as depicted in Section III-A. The traffic sources and drains are at the edge area, so that the load at the edge area is fixed and cannot be reduced by load-balancing. When load-balancing routing is simply employed in this environment to make load equal, the load at the center area may increase redundantly without reducing the load at the boundary. The redundancy induces more interference and deteriorates network performance [39], [40]. Hence, load-balancing may hurt network performance in this scenario.

In Scenario 2 (Section III-B), the load density function is constant over the domain $[0, 1)$. Straight line routing for Scenario 2 *itself* balances the relay traffic over the disk. Any efforts to balance relay load cannot perform better than straight line routing in Scenario 2. In other words, we uniformly choose a source S and a destination T on the disk perimeter so that the probability density function of angle ξ between line segments $\overline{ST}$ and $\overline{SO}$, as in Figure 12, is $\cos(\xi)$ for $0 \le \xi < \frac{\pi}{2}$. Then, the relaying load imposed by straight line routing is balanced across the disk.

In Scenario 3, the center area of the disk has heavier load than the boundary. In this case, conventional load-balancing routing can alleviate the relay load concentrated at the center even if the boundary area has more traffic. The equally distributed load can prolong the network life, which is determined by the most congested area, as in [5], [6].

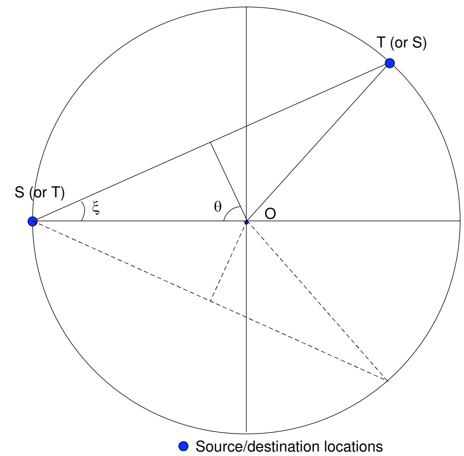

Fig. 12. An example for a load balanced traffic pattern in the case of a cluster system model. θ is half an angle $\angle SOT$. ξ is an angle between line segment $\overline{ST}$ and x-axis. The dot lines are reflections of solid line segments.

VII. CONCLUSION

In this paper, using geometric probability, we have developed an analytical model to study the performance of straight line routing for multi-hop wireless networks. Our analytical results show that the probability that a node relays a packet depends on the location of the node and the perimeter of the node's Voronoi cell. In the asymptotic region, the relaying probability at a node is approximated as the product of the half length of the perimeter of the node and the load density that the packet goes through the node's location. Both simulations and analysis show that the relay load over the network, imposed by straight line routing, depends on the model of the traffic pattern. Even if the system settings are identical and straight line routing is commonly adopted, the relay load induced by "random" traffic could be distributed differently over the network. This paradoxical result is a consequence of the famous Bertrand's paradox. Thus, in contrast to traditional belief, there are many scenarios in which straight line routing itself can balance the load over the network, and in such cases explicit load-balanced routing may not help mitigate the relaying load.

APPENDIX

We here prove (11), (13), and (14) in Section III-C.

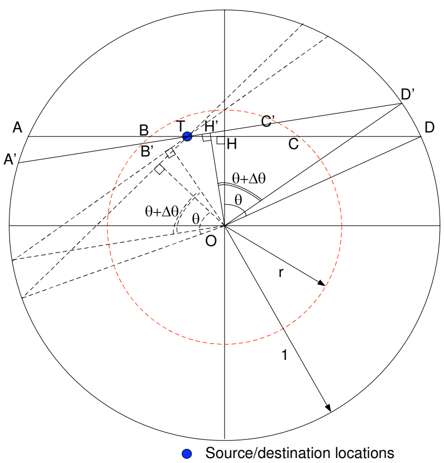

Fig. 13. In the case when Θ is defined on $[0, \frac{\pi}{2})$, there is a reflection of regions TAA' and TDD', where $\angle D'OH'$ (or $\angle A'OH'$) is $\theta + \Delta\theta$

A. Proof of (11)

Since the area of a wedge shaped region of radius r and angle θ is $\frac{1}{2}r^2\theta$, and $\Delta\beta = \frac{\sin\theta\Delta\theta}{\sqrt{z^2-\cos^2\theta}}$ from [18], for $\theta \in [0, \frac{\pi}{2})$, we have

$$\begin{aligned} & \text{Area}(\mathcal{A}\bigcup\mathcal{B}) \\ = \; & \text{Area}(\mathcal{A}) + \text{Area}(\mathcal{B}) \\ = \; & \frac{1}{2}|\overline{AT}|^2\Delta\beta + \frac{1}{2}|\overline{TD}|^2\Delta\beta \\ = \; & \frac{1}{2}\left(|\overline{AT}|^2 + \overline{TD}|^2\right)\Delta\beta \\ = \; & \frac{1}{2}\left((|\overline{AH}| - |\,\overline{TH}|)^2 + (|\overline{DH}| + |\overline{TH}|)^2\right)\Delta\beta \\ = \; & \left(|\overline{AH}|^2 + |\overline{TH}|^2\right)\Delta\beta \\ = \; & (z^2 - \cos^2\theta + \sin^2\theta)\Delta\beta \\ = \; & (z^2 - \cos^2\theta + \sin^2\theta)\frac{\sin\theta\Delta\theta}{\sqrt{z^2 - \cos^2\theta}}, \end{aligned} \tag{19}$$

where H is a middle point between points A and D, and $|\overline{TH}|$ represents the length of line segment $\overline{TH}$.

In Section III-C, the half angle Θ is defined on $[0, \frac{\pi}{2})$ (instead of $[0, \pi)$). As illustrated in Figure 13, for given node T and angles θ and $\theta + \Delta\theta$, there is a reflection of regions $TAA'(\mathcal{A})$ and $TDD'(\mathcal{B})$. Therefore, given that the first random node T, the probability that the chord going through the two random points intercepts an arc of half angle between θ and $\theta + \Delta\theta$ for $\theta \in [0, \frac{\pi}{2})$ is twice the probability that the second point S falls in two wedged regions $\mathcal{A}$ and $\mathcal{B}$.

From (19), given that the first random node T falls a distance z from the center of the unit disk, the conditional probability $\Pr[(\theta, \theta + \Delta\theta)|z]$ that we would like to get for $\theta \in [0, \frac{\pi}{2})$ is

$$\begin{aligned} & \Pr[(\theta, \theta + \Delta\theta)|z] \\ = \; & \frac{2\text{Area}(\mathcal{A}\bigcup\mathcal{B})}{\text{Area}(\mathcal{D})} \\ = \; & \frac{2}{\pi}(z^2 - \cos^2\theta + \sin^2\theta)\frac{\sin\theta\Delta\theta}{\sqrt{z^2 - \cos^2\theta}}. \end{aligned}$$

B. Proof of (13)

Similarly to Area($\mathcal{A}\bigcup\mathcal{B}$), we can express Area($\mathcal{A}_{a1}\bigcup\mathcal{B}_{a1}$) for $\theta \in [0, \frac{\pi}{2})$ in Figure 6 (a), as

$$\begin{aligned} & \text{Area}(\mathcal{A}_{a1}\bigcup\mathcal{B}_{a1}) \\ = \; & \text{Area}(\mathcal{A}_{a1}) + \text{Area}(\mathcal{B}_{a1}) \\ = \; & (\text{Area}(\mathcal{A}) - \text{Area}(\mathcal{A}_{a2})) + (\text{Area}(\mathcal{B}) - \text{Area}(\mathcal{B}_{a2})) \\ = \; & (\text{Area}(\mathcal{A}) + \text{Area}(\mathcal{B})) - (\text{Area}(\mathcal{A}_{a2}) + \text{Area}(\mathcal{B}_{a2})) \\ = \; & (z^2 - \cos^2\theta + \sin^2\theta)\Delta\beta \\ & -(z^2 - \cos^2\theta + r^2 - \cos^2\theta)\Delta\beta \\ = \; & (1 - r^2)\Delta\beta \\ = \; & (1 - r^2)\frac{\sin\theta\Delta\theta}{\sqrt{z^2 - \cos^2\theta}}, \end{aligned} \tag{20}$$

where $\mathcal{A}_{a2}$ and $\mathcal{B}_{a2}$ represent regions $BB'T$ and $CC'T$, respectively.

From (19) and (20), when the first node T falls in the circle with radius r, the conditional expectation $E[\chi_r|(\theta, \theta + \Delta\theta), z]$ of the number of points χ_r for $\theta \in [0, \frac{\pi}{2})$ is

$$\begin{aligned} E[\chi_r|(\theta, \theta + \Delta\theta), z] &= 1 \times \frac{2\text{Area}(\mathcal{A}_{a1}\bigcup\mathcal{B}_{a1})}{2\text{Area}(\mathcal{A}\bigcup\mathcal{B})} \\ &= \frac{(1 - r^2)}{(z^2 - \cos^2\theta + \sin^2\theta)}. \end{aligned}$$

C. Proof of (14)

Let angle β denote $\angle OTB$ (or $\angle OTC$) and y denote $|\overline{TB}|$ (or $|\overline{TC}|$) in Figure 6 (b). From trigonometric formula, we have

$$r^2 = y^2 + z^2 - 2yz\cos\beta.$$

Since the solution y of the above equation is

$$y = z\cos\beta \pm \sqrt{r^2 - z^2\sin\beta},$$

lengths $|\overline{TB}|$ and $|\overline{TC}|$ are expressed as

$$\begin{aligned} |\overline{TB}| &= z\cos\beta - \sqrt{r^2 - z^2\sin\beta} \\ |\overline{TC}| &= z\cos\beta + \sqrt{r^2 - z^2\sin\beta}. \end{aligned}$$

Hence, for infinitesimal $\Delta\beta$ and $0 \leq \beta \leq \arcsin(\frac{r}{z})$, Area($\mathcal{B}_{b2}$) for $\theta \in [0, \frac{\pi}{2})$ is expressed as

$$\begin{aligned} & \text{Area}(\mathcal{B}_{b2}) \\ = \; & \int_{\beta}^{\beta+\Delta\beta} |\overline{BC}|_\alpha |\text{path of } H|_\alpha d\alpha \\ = \; & |\overline{BC}|_\beta |\overline{TH}|_\beta \Delta\beta \\ = \; & 2\sqrt{r^2 - z^2\sin\beta}\,(z\cos\beta)\,\Delta\beta \\ = \; & 2\sqrt{r^2 - \cos^2\beta}\sqrt{z^2 - \cos^2\beta}\Delta\beta \\ = \; & 2\sqrt{r^2 - \cos^2\theta}\sqrt{z^2 - \cos^2\theta}\frac{\sin\theta\Delta\theta}{\sqrt{z^2 - \cos^2\theta}}, \end{aligned} \tag{21}$$

where H is the middle point of line segment $\overline{BC}$, as in Figure 6 (b), and $|\overline{BC}|_\beta$ is the length of line segment $|\overline{BC}|$ when angle $\angle OTH$ is β.

Similarly to Area($\mathcal{B}_{b2}$), we have

$$\begin{aligned}
& \text{Area}(\mathcal{B}_{b3}) \\
= & \frac{1}{2}|\overline{TD}|^2\Delta\beta - \frac{1}{2}|\overline{TC}|^2\Delta\beta \\
= & \frac{1}{2}(1 - r^2 + 2\sin\theta\sqrt{z^2-\cos^2\theta} \\
& -2\sqrt{r^2-\cos^2\theta}\sqrt{z^2-\cos^2\theta})\Delta\beta \\
= & \frac{1}{2}(1 - r^2 + 2\sin\theta\sqrt{z^2-\cos^2\theta} \\
& -2\sqrt{r^2-\cos^2\theta}\sqrt{z^2-\cos^2\theta})\frac{\sin\theta\Delta\theta}{\sqrt{z^2-\cos^2\theta}}. \quad (22)
\end{aligned}$$

From (19), (21), and (22), when the first node T falls out of the circle with radius r, the conditional expectation $E[\chi_r|(\theta, \theta+\Delta\theta), z]$ of the number of points χ_r for $\theta \in [0, \frac{\pi}{2})$ is

$$\begin{aligned}
& E[\chi_r|(\theta, \theta+\Delta\theta), z] \\
= & 1 \times \frac{2\text{Area}(\mathcal{B}_{b2})}{2\text{Area}(\mathcal{A}\bigcup\mathcal{B})} + 2 \times \frac{2\text{Area}(\mathcal{B}_{b3})}{2\text{Area}(\mathcal{A}\bigcup\mathcal{B})} \\
= & \frac{(1 - r^2 + 2\sin\theta\sqrt{z^2-\cos^2\theta})}{(z^2-\cos^2\theta+\sin^2\theta)}.
\end{aligned}$$

References

[1] S. Kwon and N. Shroff, "Paradox of shortest path routing for large multi-hop wireless networks," in *IEEE INFOCOM'07*, May 2007, pp. 1001–1009.

[2] J. M. Kahn, R. H. Katz, and K. S. J. Pister, "Mobile networking for smart dust," in *ACM MobiCom'99*, August 1999, pp. 271–278.

[3] I. F. Akyildiz, W. Sue, Y. Sankarasubarmaniam, and E. Cayirci, "A survey on sensor networks," *IEEE Communications Magazine*, vol. 40, no. 8, pp. 102–114, August 2002.

[4] I. F. Akyildiz, X. Wang, and W. Wang, "Wireless mesh networks: a survey," *Computer Networks*, vol. 47, no. 4, pp. 445–487, March 2005.

[5] L. Lin, N. B. Shroff, and R. Srikant, "Power aware routingfor multi-hop networks with energy replenishment," in *the 38th Conference on Information Sciences and Systems (CISS)*, 2004, pp. 17–19.

[6] K. Kar, M. Kodialam, T. V. Lakshman, and L. Tassiulas, "Routing for network capacity maximization in energy-constrained ad-hoc networks," in *IEEE INFOCOM'03*, April 2003, pp. 673 – 681.

[7] S. J. Lee and M. Gerla, "Aodv-br: Backup routing in ad hoc network," in *IEEE WCNC'00*, September 2000, pp. 1311–1316.

[8] A. Nasipuri, R. Castaneda, and S. R. Das, "Performance of multipath routing for on-demand protocols in mobile ad hoc networks," *Mobile Networks and Applications (MONET)*, vol. 6, no. 4, pp. 339–349, 2001.

[9] S. J. Lee and M. Gerla, "Split multi-path routing with maximally disjoint paths in ad hoc networks," in *IEEE ICC'01*, 2001, pp. 3201–3205.

[10] A. Nasipuri and S. R. Das, "On-demand multi-path routing for mobile ad hoc networks," in *IEEE ICCCN'99*, 1999, pp. 64–70.

[11] M. K. Marina and S. R. Das, "On-demand multipath distance vector routing in ad hoc networks," in *IEEE International Conference on Network Protocols (ICNP'00)*, 2000, pp. 14–23.

[12] M. K. Marina and S. R. Das, "Ad hoc on-demand multipath distance vector routing," *ACM SIGMOBILE Mobile Computing and Communications Review*, vol. 6, no. 3, pp. 92–93, 2002.

[13] M. Dong L. Zhang L.Wang, Y. Shu and O.W.W. Yang, "Multipath source routing in wireless ad hoc networks," in *Canadian Conference on Electrical and Computer Engineering*, 2000, vol. 1, pp. 479–483.

[14] M. Dong L. Zhang L.Wang, Y. Shu and O.W.W. Yang, "Adaptive multipath source routing in ad hoc networks," in *IEEE International Conference on Communications (ICC'01)*, 2001, vol. 3, pp. 867–871.

[15] P. Gupta and P. R. Kumar, "The capacity of wireless networks," *IEEE Transactions on Information Theory*, vol. 46, no. 2, pp. 388–404, 2000.

[16] M. Franceschetti, O. Dousse, D. Tse, and P. Thiran, "On the throughput capacity of random wireless networks," Preprint, Dept. of ECE, University of California, San Diego. Available at `http://fleece.ucsd.edu/~massimo/`, 2005.

[17] J. Li, C. Blake, D. D. Couto, H. Lee, and R. Morris, "Capacity of ad hoc wireless networks," in *ACM MobiCom'01*, July 2001, pp. 61–69.

[18] H. Solomon, *Geometric Probability*, Society for Industrial and Applied Mathematics, Philadelphia, PA, 1978.

[19] P. P. Pham and S. Perreau, "Increasing the network performance using multi-path routing mechanism with load balance," *Ad hoc Networks*, vol. 2, no. 4, pp. 433–459, 2004.

[20] Y. Ganjali and A. Keshavarzian, "Load balancing in ad hoc networks: Single-path routng vs. multi-paht routing," in *IEEE INFOCOM'04*, March 2004, vol. 2, pp. 1120–1125.

[21] E. Hyytia, P. Lassila, and J. Virtamo, "Spatial node distribution of the random waypoint mobility model with applications," *IEEE Transactions on Mobile Computing*, vol. 5, no. 6, pp. 680–694, June 2006.

[22] R. Negi and A. Rajeswaran, "Capacity of power constrained ad-hoc networks," in *IEEE INFOCOM'04*, March 2004, vol. 1, pp. 7–11.

[23] D. P. Dobkin, S. J. Friedman, and K. J. Supowit, "Delaunay graphs are almost as good as complete graphs," *Discrete and Computational Geometry*, , no. 5, pp. 399–407, 1990.

[24] D. Stoyan, W. S. Kendall, and J. Mecke, *Stochastic Geometry and Its Applications*, John Wiley and Son, New York, 2nd edition, 1995.

[25] A. Papoulis, *Probability, Random Variables, and Stochastic Process*, McGraw-Hill, New York, 3rd edition, 1991.

[26] S. Bandyopadhyay and E. J. Coyle, "An energy efficient hierarchical clustering algorithm for wireless sensor networks," in *IEEE INFOCOM'03*, April 2003, vol. 3, pp. 1713–1723.

[27] P. Jacquet, "Geometry of infromation propagation in massively dense ad hoc networks," in *ACM MobiHoc'04*, May 2004, vol. 1, pp. 157–162.

[28] W. B. Heinzelman, A. P. Chandrakasan, and H. Balakrishnan, "An application-specific protocol architecture for wireless microsensor networks," *IEEE Transactions on Wireless Communications*, vol. 1, no. 4, pp. 660–670, 2002.

[29] A. M. Mathai, *An Introduction to Geometrical Probability: Distributional Aspects with Applications*, Gordon and Breach Science Publishers, Amsterdam, the Netherlands, 1978.

[30] S. Boyd and L. Vandenberghe, *Convex Optimization*, Cambridge University Press, Cambridge, United Kingdom, 2004.

[31] E. W. Weisstein, "Disk point picking," From MathWorld–A Wolfram Web Resource. http://mathworld.wolfram.com/DiskPointPicking.html.

[32] E. K. P. Chong and S. H. Zak, *An Introduction to Optimization*, John Wiley and Sons, Inc., New York, 2nd edition, 2001.

[33] S. Ross, *Stochastic Process*, John Wiley and Sons, Inc., New York, 2nd edition, 1996.

[34] A. L. Hinde and R. E. Miles, "Monte carlo estimates of the distributions of the random polygons of the voronoi tessellation with respect to a poisson process," , no. 10, pp. 205–223, 1980.

[35] D. M. Blough and P. Santi, "Investigating upper bounds on networks lifetime extension for cell-based energy conservation tehniques in stationary ad hoc networks," in *ACM MobiCom'02*, September 2002, vol. 1, pp. 183–192.

[36] J. H. Chang and L. Tassiulas, "Energy conserving routing in wireless ad-hoc networks," in *IEEE INFOCOM'00*, 2000, vol. 1, pp. 22 – 31.

[37] L. Lin, N. B. Shroff, and R. Srikant, "Asymptotically optimal power-aware routing for multihop wireless networks with renewable energy sources," in *IEEE INFOCOM'05*, March 2005, vol. 2, pp. 1262–1272.

[38] J. Gao and L. Zhang, "Load balanced shortest path routing in wireless networks," in *IEEE INFOCOM'04*, March 2004, vol. 2, pp. 1098–1107.

[39] S. Kwon and N. Shroff, "Energy-efficient interference based routing for multi-hop wireless networks," in *IEEE INFOCOM'06*, April 2006.

[40] S. Kwon and N. Shroff, "Unified energy-efficient routing for multi-hop wireless networks," in *IEEE INFOCOM'08*, April 2008, pp. 430–438.

Sungoh Kwon (S'05 / M'08) received his B.S. and M.S. degrees in electrical engineering from KAIST, Daejeon, Korea, and the Ph.D. degree in electrical and computer engineering from Purdue University, West Lafayette, IN, in 1994, 1996, and 2007, respectively. From 1996 to 2001, he had worked as a research staff in Shinsegi Telecomm Inc., Seoul, Korea. He is now with Samsung Electronics Co., LTD, Korea. His research interests are in wireless communication networks.

Ness B. Shroff (S'91 / M'93 / SM'01/ F'07) is currently the Ohio Eminent Scholar of Networking and Communications, and Professor of ECE and CSE at The Ohio State University. Previously, he was a Professor of ECE at Purdue University and the director of the Center for Wireless Systems and Applications (CWSA), a university-wide center on wireless systems and applications. His research interests span the areas of wireless and wireline communication networks, where he investigates fundamental problems in the design, performance, pricing, and security of these networks.

Dr. Shroff has received numerous awards for his networking research, including the NSF CAREER award, the best paper awards for IEEE INFOCOM'06 and IEEE INFOCOM'08, the best paper award for IEEE IWQoS'06, the best paper of the year award for the Computer Networks journal, and the best paper of the year award for the Journal of Communications and Networks (JCN) (his IEEE INFOCOM'05 paper was one of two runner-up papers).